Study of Structural, Electrical, and Dielectric Properties of Polystyrene/Foliated Graphite Nanocomposite Developed Via *In Situ* Polymerization

N. K. Srivastava, R. M. Mehra

Department of Electronic Science, University of Delhi South Campus, New Delhi 110 021, India

Received 2 January 2008; accepted 30 March 2008
DOI 10.1002/app.28499
Published online 10 June 2008 in Wiley InterScience (www.interscience.wiley.com).

ABSTRACT: Present article reports the investigations of the electrical and dielectric properties of polystyrene/foliated graphite (PS/FG) nanocomposites. The homogenous embedded structure of FG within the polymer matrix has been confirmed by scanning electron microscopy (SEM). The electrical conductivity of the composite was found to exhibit insulator–conductor transition at a very low percolation threshold of FG. A nonlinear to linear transition in the current–voltage characteristics of the composites was observed when the composite undergoes insulator–conductor transition. The frequency dependence of dielectric constant, dissipation factor, and ac conductivity has also been analyzed using percolation theory. D-shore hardness of the nanocomposite was also tested to observe the strength of the composites. © 2008 Wiley Periodicals, Inc. J Appl Polym Sci 109: 3991–3999, 2008

Key words: polystyrene; nanocomposites; dielectric properties; hardness

INTRODUCTION

Most of the polymeric materials are electrically insulating in nature. These insulating polymers can be made electrically conductive by suitably incorporating conducting fillers as a second phase into these matrices, leading to increase in the electrical conductivity of the resulting composites.[1,2] The electrical and dielectric properties of these composites are mainly dependent on the filler content. When the filler content reaches a certain critical value, the so-called percolation threshold, an insulator-to-conductor transition in the conductivity of the composites occurs.[3,4] Simultaneously, there is a sharp transition in the dielectric properties of the composites.

Natural flake graphite (NFG),[5,6] carbon black,[7,8] and metal powders[9,10] have been commonly used as conducting fillers in the polymer composites. Recently, Chen et al.[11] has developed an *in situ* polymerization process to fabricate polystyrene/expanded graphite by polymerization of styrene in the presence of expanded graphite in the forms of nanosheets. It has been shown by them that expanded graphite can also act as good conducting filler for polymers without affecting the d-spacing of carbon layers after polymerization. The fabrication of expanded graphite with intercalation kinetics had been initially reported by Chung,[12] Anderson and Chung,[13] etc.

The dielectric constant of individuals for either polymer[14,15] and/or fillers[16] is in the range of 2–15. However, an abrupt increase in the value of dielectric constant and dissipation factor values has been reported in such composites around the percolation concentration of filler and explained in terms of trapping of charge carriers in various insulating–conducting interfaces formed within the composites.[17,18] Fabrication of the composites having high dielectric constant and low losses is very demanding nowadays as they can be used as embedded capacitors and effectively used in multiple functions such as decoupling, by-passing, filtering, and timing capacitors. Embedded capacitors require very high capacitance density because of the limit in their capacitor area along with low temperature fabrication process. The overall benefits of embedded capacitors are reduction in the costs of the capacitors, easy placement, more reliable, better performing, cost effective capacitor material, and miniaturization of electronic systems. The dielectric properties of the composites depend on the volume fraction, size and shape of conducting fillers, preparation method, interface and interaction between the fillers, and the polymer. It is, therefore, an interesting aspect to analyze the dielectric properties of the polymer/FG nanocomposite as a function of filler content and frequency.

Correspondence to: R. M. Mehra (rammehra2003@yahoo.com).
Contract grant sponsor: DRDO, Government of India.
Contract grant sponsor: ERIP/ER/0503529/M/01/850.
Contract grant sponsor: University of Delhi, Delhi.

In this article, polystyrene/foliated graphite (PS/FG) nanocomposites were prepared via *in situ* polymerization technique. The composites were characterized using X-ray diffraction (XRD), Fourier transforms infra-red spectroscopy (FTIR), and scanning electron microscopy (SEM). SEM images of the composites revealed an embedded structure with fine spatial homogeneity of FG into the polymer matrix. Electrical conductivity (dc) and current–voltage (I–V) characteristics of PS/FG composites were investigated as a function of filler volume fraction. The I–V characteristics were correlated with the SEM images of the nanocomposite. Percolation threshold of filler was estimated using power law model and was further confirmed by four parameter computer fitting of generalized effective media (GEM) equation. Dielectric constant, dissipation factor, and ac conductivity of these composites were also analyzed as a function of FG and frequency with highlighting the effect of onset of percolation threshold concentration of filler. Scaling behavior was also observed in dielectric constant versus filler content data similar to the conductivity data. Effect of percolation on various dielectric properties was summarized and correlated with the electrical dc conductivity of the composites. The strength of these composites was estimated in terms of D-shore hardness.

EXPERIMENTAL

Materials

PS was prepared by *in situ* polymerization using styrene monomer (Alfa Acer, USA). The glass transition temperature (T_g) of PS was determined using differential scanning calorimetry and was found to be 100°C. The source of conducting filler was NFG with average particle size of 10–20 μm supplied by Graphite India Ltd. Conductivity of the graphite flakes was 1.33×10^4 S/cm with density 1.75 g/cm^3. NFG was used to fabricate the FG. By using FG as conducting filler, PS/FG samples have been developed. Concentrated sulfuric and nitric acids were used as acid-intercalates to prepare graphite-intercalated compound (GIC). Benzoyl peroxide (BPO) (Merck E., Germany) was used as initiator in the polymerization process.

Preparation of foliated graphite

Initially, before the preparation of nanocomposite, FG was prepared using NFG as reported in the literature.[19] Graphite flake is a layered structure of carbon, where the carbon atoms are bonded with weak van der Waals forces between the layers. NFG can be intercalated by exposure to an appropriate chemical reagent. Mixture of concentrated sulfuric and nitric acid (4 : 1 v/v) was mixed with graphite flakes at room temperature and stirred continuously for 16 h. The acid-treated natural graphite flake was first neutralized with water and then vacuum filtered followed by drying at 100°C to remove the remaining moisture. The dried particles are known as GIC. Acid-intercalated ions occupy the space in between the carbon layers during the formation of GIC. The exfoliation of GIC can be achieved by providing a thermal shock in microwave oven for 20 s to obtain exfoliated graphite (EG). There is a sudden expansion about hundreds of times along their *c*-axis during exfoliation, forming worm-like shapes. EG, a loose and porous vermicular product of greatly decreased density, was then immersed in 70% aqueous alcohol solution and subjected to sonication in an ultrasonic bath for 8 h. The resulting dispersion was vacuum filtered and dried to obtain FG. From the SEM image of FG in Figure 1, the shape of FG was found to be like sheets with average thickness and diameter as 80–150 nm and 5–10 μm, respectively.

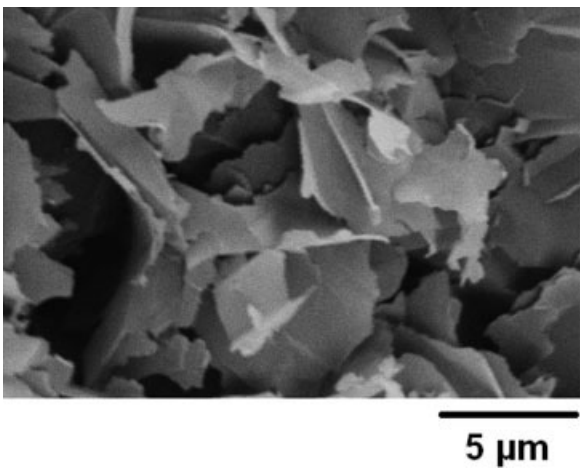

Figure 1 Scanning Electron Micrograph of foliated graphite.

In situ polymerization

Initially, various ratio of FG was mixed with styrene in a tightly sealed test tube. The test tube was subjected to sonication in the ultrasonic bath for 20 min at temperature of 60°C to provide proper dispersion of FG into the monomer. Sonication was continued with the addition of the initiator BPO (0.5 wt % of monomer) into the mixture at 80°C for 10–12 h till the suspension turns into a black solid. It was ensured in the polymerization setup that constant heating was provided to the mixture along with continuous sonication till the end of polymerization process. Constant heating provides uniform polymerization rate , whereas constant sonication is required for better dispersion of FG into the gradually polymerizing solution. From the black solid, circular samples were cut down for the measurement purpose.

The density of the pure PS pellet and FG were found to be 0.988 g/cm^3 and 1.975 g/cm^3, respectively. Series of disk-shaped specimens of PS/FG conductive composites with varying filler contents from 0 to 0.031 volume fraction of GN were prepared.

Characterization and measurements

Both surfaces of the pellets were polished with sandpaper to remove the rich polymer surface layer and to eliminate surface irregularities. The conducting silver paint ''Conductrox 3347 AG conductor" coatings supplied from ferro-electric materials, USA, was used as the electrical contact. Pellets were sealed in air-free polyethylene bags before testing to avoid atmospheric and humidity effects. XRD measurements were done using CuKα radiation (λ = 0.154 nm) operated at 40 kV and 40 mA in the 2θ range of 20−80°. Infrared spectra were recorded on a Perkin–Elmer 102 FTIR spectrometer. The samples for FTIR measurement have been prepared using KBr (Alfa Acer, USA). Before preparing the samples for FTIR, KBr was kept in an oven at 50°C to remove any moisture. KBr was mixed mechanically by pastel mortar with required materials in 100 : 2 ratio (wt %) followed by simple compression molding with 105 MPa at room temperature for 10 min. Scientico Hardness tester (Durometer, model No. SRHT-501D) conforming to ASTM 1706-61 and D 676-59T specifications was used to determine the hardness of the samples. Pellets of ~0.5 cm thickness have been taken for accurate and reliable results of hardness measurement. A digital multimeter was used for samples having electrical resistance lower than 200 MΩ. However, for the samples having resistance greater than 200 MΩ, a Keithley Pico ammeter (Model DPA III) was used. Current–voltage measurements were performed by Keithley 2400 source meter. The LEO 435 VP field emitting scanning electron microscope was used for the analysis of morphology of the FG and composite polymer. Measurement of capacitance and dissipation factor of the composites was carried out with an impedance analyzer (HP-4294 A) within the frequency range of 20 Hz to 5 MHz.

RESULTS AND DISCUSSION

X-ray diffraction analysis

X-ray diffraction (XRD) pattern of pure FG, pure PS, and PS/FG composites having 0.015 and 0.031 volume fraction of FG is shown in Figure 2(a–d), respectively. It is seen from Figure 2(a) that pure FG exhibits a strong *c*-axis oriented 002 peak at angle 2θ = 26.78°. The full width at half maxima (FWHM) is found to be 0.240°. The grain size and the d-spacing was estimated to be 35 nm (using Scherrer's relation[20]) and 3.325 Å for pure FG. No peak was found for pure PS in the XRD pattern [Fig. 2(b)]. The XRD peaks, for the nanocomposites with two different filler concentration, were observed at angle 2θ = 26.53° [Fig. 2(c,d)]. The d-spacing value for the composites was estimated to be 3.355 Å, which is close to the value observed for pure FG. This shows that there is no increase in the spaces between the graphite layers and no change in the crystalline structure of graphite due to polymerization.

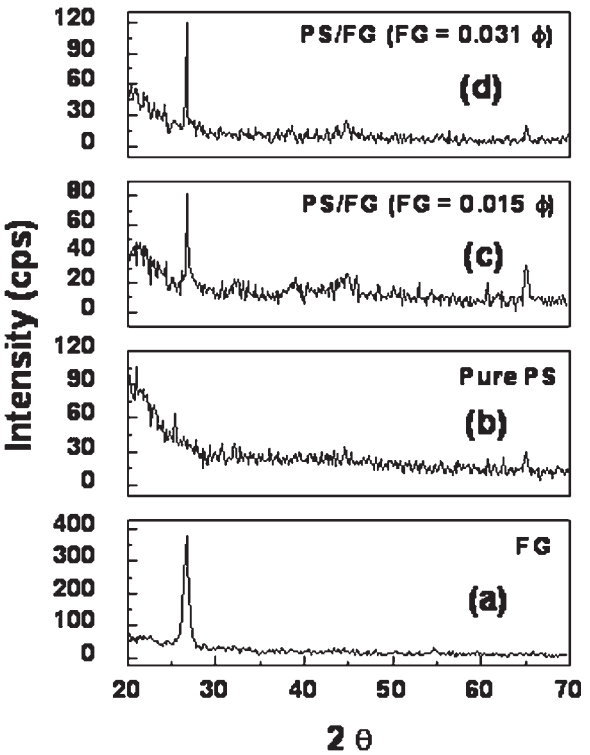

Figure 2 X-ray diffraction patterns of (a) foliated graphite, (b) pure PS, (c) PS/FG (ϕ = 0.015 volume fraction), and (d) PS/FG (ϕ = 0.031 volume fraction).

Fourier transforms infra-red spectroscopy

The FTIR spectrum of the obtained pure PS after polymerization and PS/FG nanocomposite for 0.005 volume fraction of FG is shown in Figure 3. The characteristic absorption bands of PS are revealed from the FTIR spectra. The PS characteristic bands[21] are aromatic CH stretching (3027, 3061 cm^{-1}), CH_2 asymmetric stretching (2925 cm^{-1}), CH_2 symmetric stretching (2854 cm^{-1}), C—C in-plane vibration (1601 cm^{-1}, 1494 cm^{-1}, 1453 cm^{-1}), CH out-of-plane bending of the phenyl ring (756, 698 cm^{-1}) and out-of-plane deformation of the phenyl ring (540 cm^{-1}). The characteristic bands are coming from almost the entire spectra range from 400 to 3500 cm^{-1}. The spectra confirm the fabrication of PS using *in situ* polymerization technique. Similar peaks at the same wavelength were observed for the nanocomposite FTIR with 0.005 volume fraction of FG as in case of

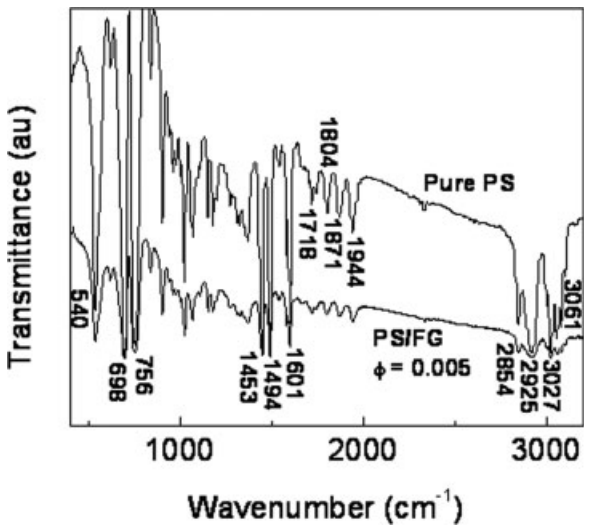

Figure 3 FTIR spectra of (a) pure PS and (b) PS/FG nanocomposite ($\phi = 0.005$ volume fraction).

pure PS. The intensity of the transmittance reduces in case of the nanocomposite due to the addition of FG in pure PS. It was difficult to obtain FTIR spectra for higher composition of FG because the intensity of transmittance reduces to a very low level.

Electrical conductivity

The electrical conductivity (σ) of FG filled PS nanocomposites as a function of FG volume fraction (ϕ) is illustrated in Figure 4. It is seen from the figure that σ increases by more than six orders when the graphite content reaches 0.01 volume fraction (2 wt %) of FG. The electrical conductivity reached 10^{-3} S/cm at a graphite content of 0.02 volume fraction (4 wt %) and thereafter saturation in conductivity was observed for higher concentration of filler.

Power law model

The conductivity data with FG volume fraction was analyzed using the power law model. The variation of σ as a function of filler content is usually explained by power law model of conductivity[22–24] where σ is expressed as

$$\sigma = \sigma_0(\phi - \phi_c)^t \tag{1}$$

where t is the universal exponent determining the power of the electrical conductivity increase above percolation threshold concentration (ϕ_c) of filler i.e., $\phi > \phi_c$ and σ_0 is generally considered to be the conductivity of the conducting filler.[24,25] From the best linear fit of the conductivity with excessive volume fraction of filler, both t and σ_0 can be obtained. The plot of log σ versus log $(\phi - \phi_c)$ is shown in the inset of Figure 4. The best linear fit was found for $\phi_c = 0.011$ volume fraction of graphite with minimum standard deviation ($\delta = 0.185$ in %). The values of t and σ_0 as estimated from the slope and intercept of the line respectively, from the inset of Figure 4 were found to be 3.07 and 1484.91 S/cm, respectively. The value of σ_0 is nearly one tenth of the conductivity of filler particles (13,333 S/cm). The observed value of $t = 3.07$ is higher than the value predicted by the power law model. Liu et al.[26] has also found large t values for polyurethanes and single walled carbon nanotubes system. Wang and Rubner[27] have also reported the value of $t = 3.2$ for their system. It may be mentioned that several research workers[22,28] have considered σ_0 as a prefactor of conductivity and obtained values which also generally do not correspond to the conductivity of the filler.

Analysis using GEM equation

To investigate the effect of filler content on the electrical conductivity of the composite more critically, McLachlan postulated GEM equation[29,30] for the binary composite polymer system. The GEM equation is written as

$$\frac{f(\sigma_{ps}^t - \sigma^t)}{\sigma_{ps}^t + A\sigma^t} + \frac{\phi(\sigma_{fg}^t - \sigma^t)}{\sigma_{fg}^t + A\sigma^t} = 0 \tag{2}$$

where σ, σ_{ps} and σ_{fg} are the conductivities of the polymer composite, the polymer matrix (PS), and the conducting filler (graphite nanosheets), respectively; f and ϕ are volume fractions of the polymer and conducting filler, thus $f + \phi = 1$. A is defined as

$$A = \frac{(1 - \phi_c)}{\phi_c} = \frac{f_c}{(1 - f_c)} \tag{3}$$

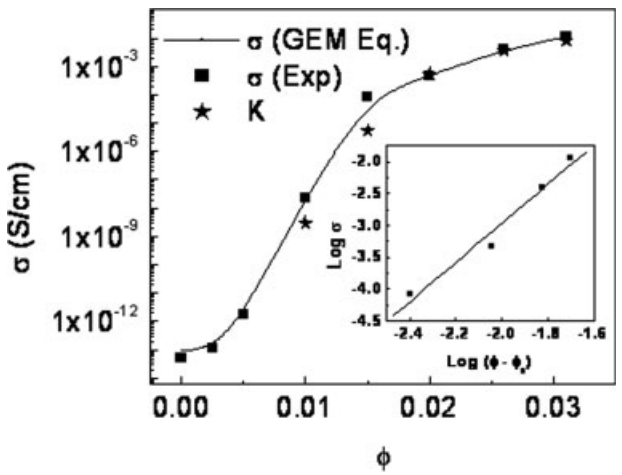

Figure 4 Variation of electrical conductivity as a function of filler content for PS/FG nanocomposite compared with GEM conductivity and K and in the inset plot of log σ versus log $(\phi - \phi_c)$ for PS/FG nanocomposite.

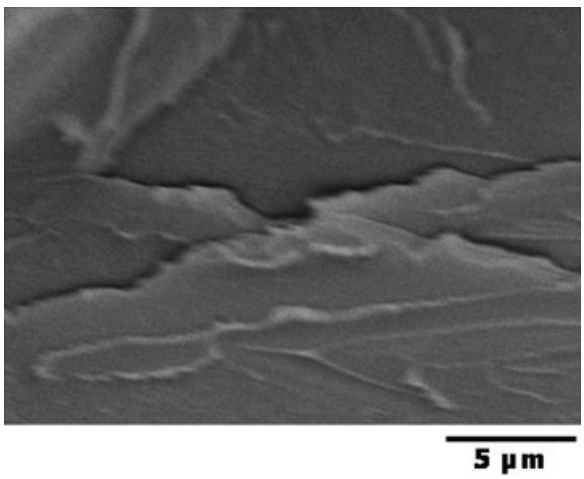

Figure 5 Scanning electron micrograph of freeze-fractured PS/FG nanocomposite for pure PS at 5000 magnification.

Using four-parameter computer fitting program, t, ϕ_c, σ_{ps}, and σ_{fg} were evaluated from the best fitting. The composite conductivity with filler concentration as estimated from the GEM equation was further compared with the experimental conductivity. The data is also shown in Figure 4. The percolation threshold concentration of filler ϕ_c was observed at 0.011 volume fraction of FG from the four parameter fittings of the GEM equation with the minimum standard deviation (δ = 0.34 in %). The observed value of ϕ_c from both the power law model and GEM equation is almost same content of filler and is close to the experimental 0.01 volume fraction (2 wt %) sample. The value of t as estimated from the four parameter fittings is 2.47 which is closer to the universal value (between 1.5 and 2) of the exponent.[22,31,32] The value of σ_{ps} and σ_{fg} was estimated to be 6.09×10^{-14} S/cm and 140.84 S/cm, respectively.

Morphology of nanocomposite

Figure 5 shows the SEM image of pure PS as prepared after polymerization at 5000 magnification. The figure indicates the uniform structure of PS with no evidence of grain boundaries. Figure 6(a–c) shows the SEM images of PS/FG nanocomposite having $\phi < \phi_c$, $\phi \sim \phi_c$, and $\phi > \phi_c$, respectively, at 4000 magnification. The SEM images [Fig. 6(b,c)] show the formation of a conducting network with homogeneous dispersion of FG into the polymer matrix. It is clearly seen from Figure 6(a) that there is a considerable distance between two FG particles for $\phi < \phi_c$. At $\phi \sim \phi_c$, [Fig. 8(c)], the filler particles are close to one another. For higher concentration of the filler $\phi > \phi_c$, the filler particles are either very close or in direct contact with each other as is seen in Figure 6(c). These micrographs of PS/FG nanocomposites also confirm the nanosheets type structure of FG after *in situ* polymerization. It may be mentioned that there was no change in the d-spacing of FG after the polymerization.

Current–Voltage characteristics

I–V characteristics can be expressed as[33]

$$1 = KV^{n} \tag{4}$$

where K represents the conductivity of the nanocomposite and n is the slope in the log I-log V plot. In eq. (4), Ohm's law is fulfilled in the system at $n = 1$. Figure 7(a–d) illustrates the I–V plots of PS/FG nanocomposite with different composition of filler. The nonlinear behavior in I–V curves is clearly seen from the Figure 7(a–c) corresponding to ϕ = 0.01, 0.02, and 0.026, respectively. The value of n for these composites was found to decrease from 1.48 to 1.19. A value of $n > 1$ represents conduction due to tunneling of charge carriers.[34] The value of n for ϕ = 0.031 was found to be 1.01, which signifies the ohmic conduction. At this value of ϕ, the filler particles are very close or in direct contact with one another as confirmed from the SEM image [Fig. 6(c)]. The transition of the conduction mechanism from nonlinear to linear is generally understood in terms of the

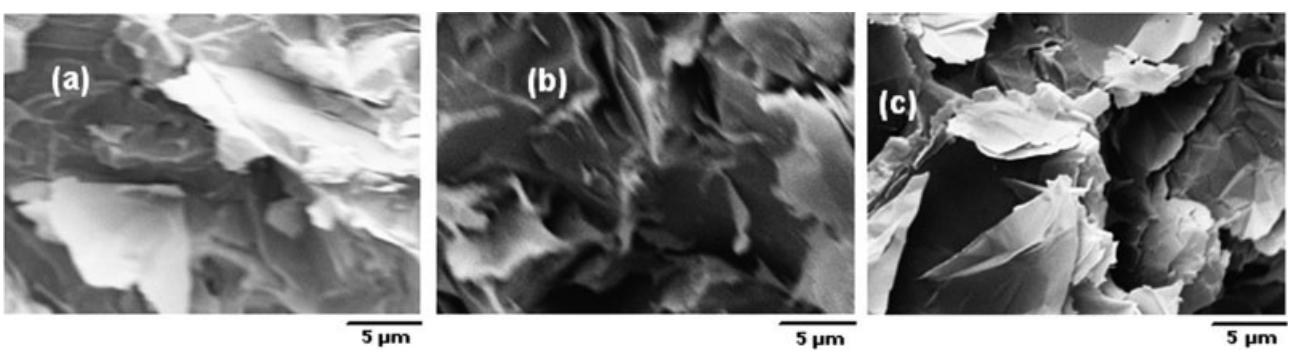

Figure 6 Scanning electron micrograph of freeze-fractured PS/FG nanocomposite for (a) ϕ = 0.005, (b) ϕ = 0.01, and (c) ϕ = 0.031 at 4000 magnification.

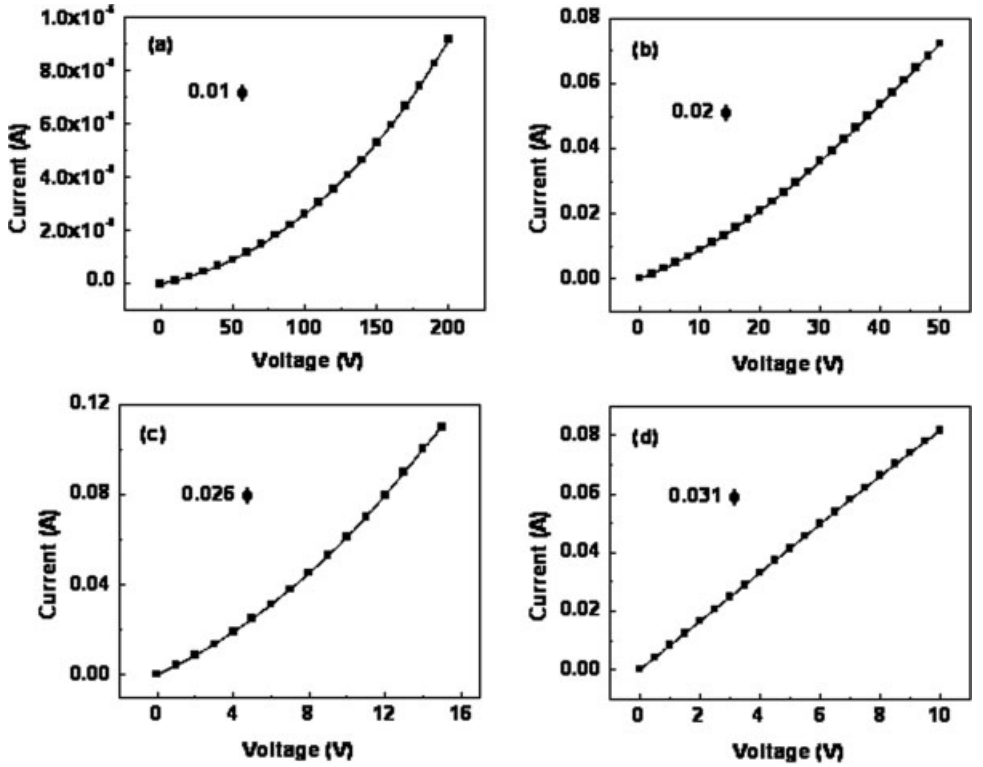

Figure 7 I–V characteristics of PS/FG nanocomposites for various ϕ as (a) 0.01, (b) 0.02, (c) 0.026, and (d) 0.031 volume fraction.

decrement of the distance and number of tunneling gaps in the percolating network. The variation of K and σ with ϕ is also shown in Figure 4. It is seen from the figure that both K and σ closely match with each other.

Dielectric properties

The large enhancement in dielectric constant around percolation threshold is also generally observed similar to the electrical conductivity of the composites. Such behavior of dielectric constant can also be explained in terms of scaling behavior of the real part of permittivity. The complex dielectric constant is a function of frequency (f) and is defined by

$$\varepsilon(\omega) = \varepsilon'(\omega) - j\varepsilon''(\omega) \quad (5)$$

where $\omega = 2\pi f$ is angular frequency of the measuring electric field. The real part $\varepsilon'(\omega)$ is usually expressed as relative permittivity or dielectric constant and imaginary part $\varepsilon''(\omega)$ generally referred as loss factor. The dissipation factor tan δ is expressed as the ratio of $\varepsilon''(\omega)$ to $\varepsilon'(\omega)$. The power law

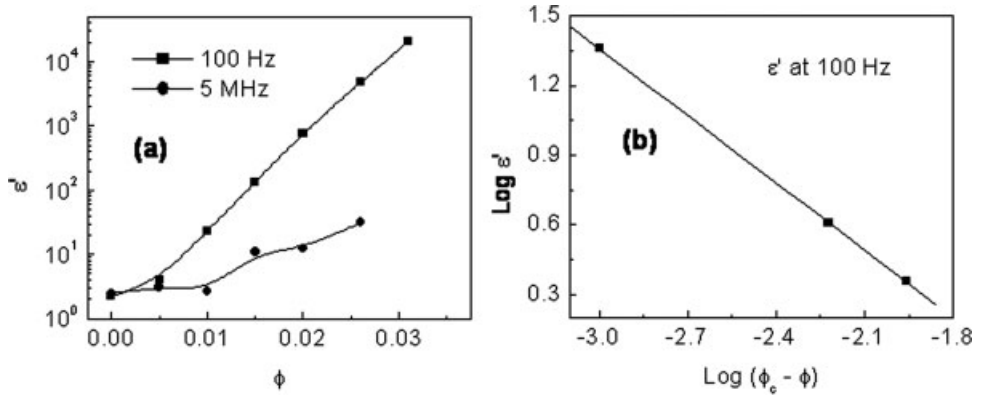

Figure 8 (a) Variation of ε' as a function of ϕ at 100 Hz and 5 MHz for PS/FG nanocomposites and (b) log–log plot of ε' versus ($\phi_c - \phi$) for PS/FG nanocomposites.

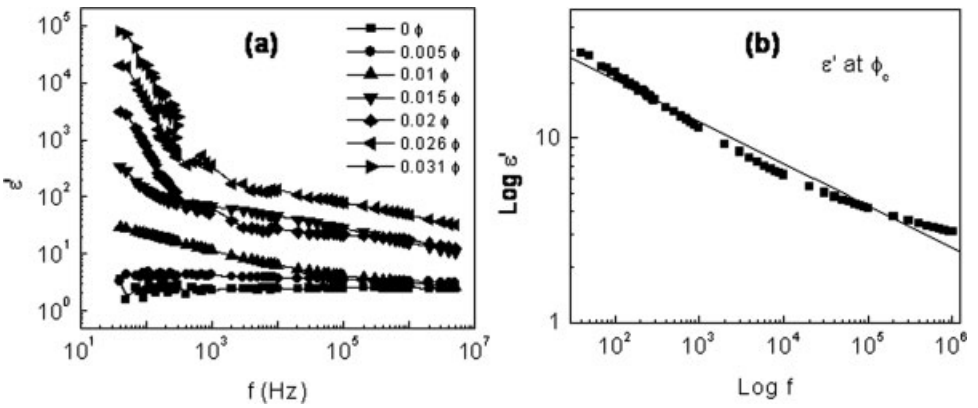

Figure 9 (a) Variation of ε' as a function of f for various ϕ for PS/FG nanocomposites and (b) log–log plot of ε' versus f at ϕ_c concentration of FG for PS/FG nanocomposites.

expresses the enhancement of the dielectric constant near the percolation threshold as follows:[35,36]

$$\varepsilon' \propto (\phi_c - \phi)^s \tag{6}$$

where s is the corresponding critical exponent of the insulating region ($\phi < \phi_c$). Figure 8(a) shows the variation of ε' as a function of FG content at two different frequencies, 100 Hz and 5 MHz. At 100 Hz, the value of ε' at ϕ_c is found to be $\sim$ 12 followed by a large increase in ε'. A maximum value of $\varepsilon' = 7.87 \times 10^4$ is obtained for $\phi = 0.031$. However, at high frequency, comparatively small increase in ε' is observed. The log–log plots of eq. (6) are shown in Figure 8(b). The value of ϕ_c and the critical exponent s are found to be 0.011 and 0.96, respectively. The value of ϕ_c is found to be the same as obtained from the power law model and GEM equation analysis of the conductivity data. The observed value of s is in good agreement with the universal ones ($S \sim 1$).[35,37,38]

The frequency variation of dielectric constant near ϕ_c as predicted by percolation theory[35] is

$$\varepsilon'(f, \phi_c) \propto f^{-v} \tag{7}$$

where v is the corresponding critical exponent. Figure 9(a) shows the dependence of ε' of PS/FG nanocomposite on the frequency for various ϕ. For $\phi < \phi_c$, ε' is insensitive to frequency variation. An increase in the value of ε' is observed around ϕ_c and for $\phi > \phi_c$, ε' is strongly dependent on frequency. Very large enhancement in the values of ε' has been obtained for lower frequency components. Such large values of ε', in the vicinity of ϕ_c, could be attributed to Maxwell–Wagner[14] interfacial polarization in heterogeneous composite systems. Because of the interfacial polarization, large local fields are generated within the composite, which results in the large value of ε' for higher composition of FG. The reason behind the large ε' at low frequencies is probably due to the follow-through of the polarization of the dipoles towards the change of the electric field, which is possible only at lower frequencies. The log–log plot of eq. (7) has been shown in Figure 9(b). The value of v, as estimated from the slope of the line from Figure 9(b), is found to be 0.23.

Variation of tan δ as a function of frequency for different values of ϕ for PS/FG nanocomposite is shown in Figure 10. Strong frequency dependence of tan δ was observed for $\phi > \phi_c$, similar to ε'. At a given frequency, considerable increase in tan δ was observed for $\phi > \phi_c$. An increase in dissipation factor was observed in between the frequency range from 100 Hz to 10 kHz beyond ϕ_c forming a camel-type structure and is found to be the maximum near 1 kHz. Such behavior of tan δ can also be explained by Maxwell–Wagner polarization. The high dissipation factor near 1 kHz may be considered as the evidence of the large leakage current in the PS/FG nanocomposite.

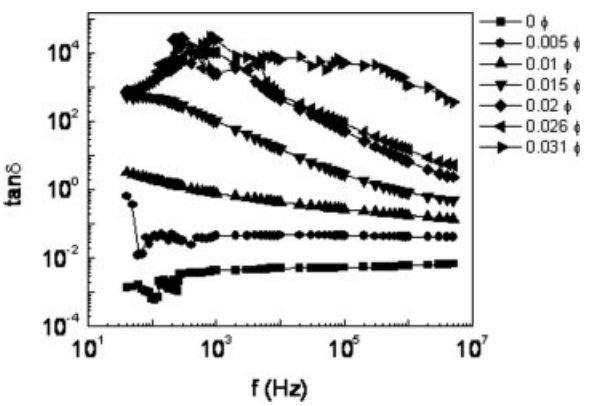

Figure 10 Variation of tan δ as a function of f for various ϕ for PS/FG nanocomposites.

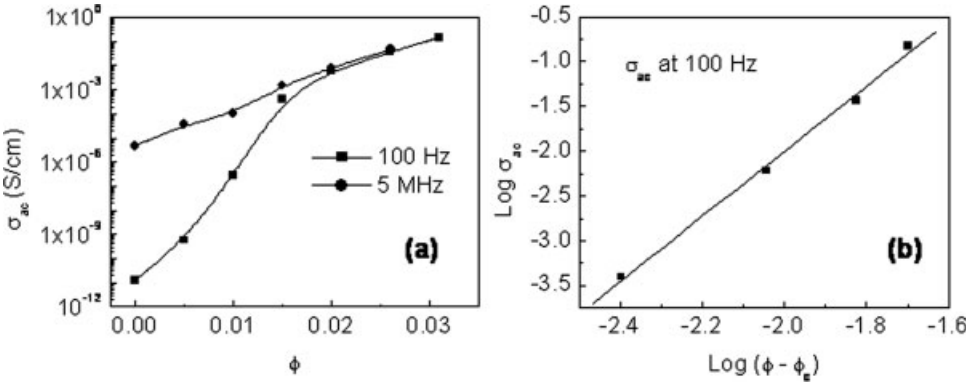

Figure 11 (a) Variation of σ_{ac} as a function of ϕ at 100 Hz and 5 MHz for PS/FG nanocomposites and (b) log–log plot of σ_{ac} versus $(\phi - \phi_c)$ for PS/FG nanocomposites.

AC conductivity

The dependence of the ac conductivity (σ_{ac}) of the PS/FG nanocomposite on ϕ for two different frequencies (100 Hz and 5 MHz) is shown in Figure 11(a). The ac conductivity is found to increase with increase in ϕ. However, large increase in σ_{ac} is found for lower frequency values. The nature of increase in σ_{ac} is similar to the dc conductivity. According to the percolation theory, the increase in σ_{ac} around ϕ_c may be expressed as following:

$$\sigma_{ac} \propto (\phi - \phi_c)^{t'} \tag{8}$$

where t' is the corresponding critical exponent. The log–log plot of eq. (8) is shown in Figure 11(b). The value of ϕ_c was observed to be the same as 0.011 volume fraction of FG. The value of t' was found to be 3.62, which is much higher as compared with the universal value of exponent. The variation of σ_{ac} with frequency of the PS/FG nanocomposite for various ϕ is shown in Figure 12(a). An increase in the ac conductivity was observed with increase in frequency upto ϕ_c. However, for higher composition of FG, the σ_{ac} was almost insensitive to frequency variation. According to the percolation theory[35] around ϕ_c, the σ_{ac} may be expressed as:

$$\sigma_{ac}(f, \phi_c) \propto f^u \tag{9}$$

where u is the corresponding critical exponent. Log–log plot of eq. (9) is shown in Figure 12(b). From the slope of the line, the value of u was found to be 0.53, which is inconsistent with the universal value[35] of 0.7. It may be mentioned that the linear fit using eq. (9) did not fit well with the ac conductivity data at ϕ_c, resulting in a lower value of u. The critical exponent's u [eq. (9)] and v [eq. (7)] are related as[35] $u + v \approx 1$. In the present system for PS/FG nanocomposite, $u + v$ turn out to be 0.76. Thus, although the variation of dielectric constant with frequency exhibits percolative nature, the ac conductivity does not show such a behavior.

D-shore hardness

D-shore hardness of PS/FG nanocomposite with respect to FG content is shown in Figure 13. A relatively fast decrease in D-shore hardness with increasing filler content was observed when the filler concentration is roughly up to the percolation concentration. A moderate decrease in hardness, however, was observed beyond percolation threshold. The decrease in hardness with increase in filler content may be assumed to be due to the gradually insuffi-

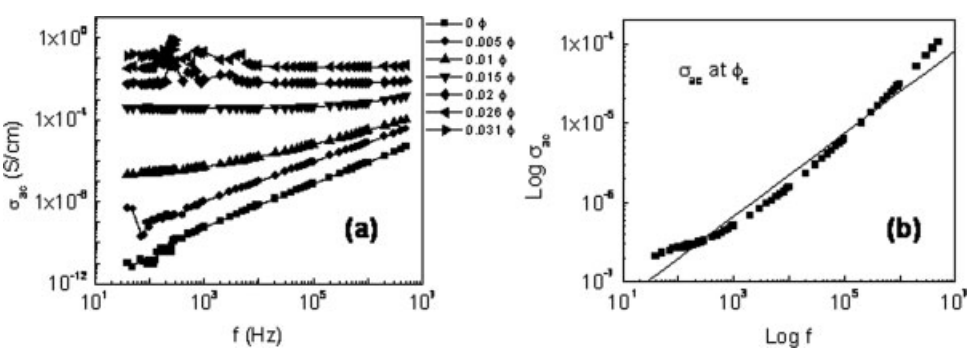

Figure 12 (a) Variation of σ_{ac} as a function of f for various ϕ for PS/FG nanocomposites and (b) log–log plot of σ_{ac} versus f at ϕ_c concentration of FG for PS/FG nanocomposites.

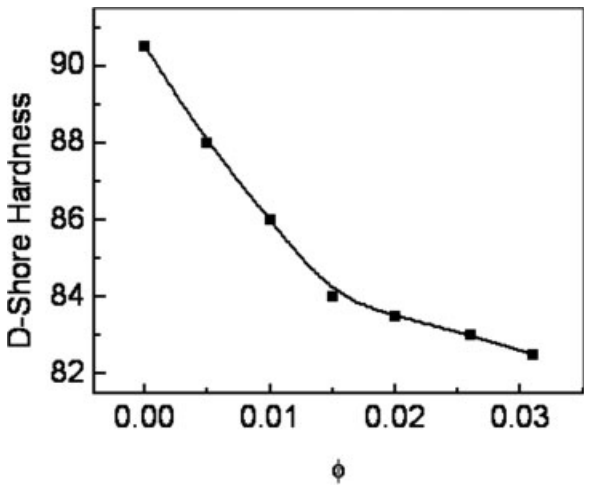

Figure 13 D-Shore hardness as a function of ϕ for PS/FG nanocomposites.

cient polymerization of the polymer matrix because of the relatively better dispersion of FG particles within the composite. It may be also mentioned here that for further higher composition of filler ($\phi > 0.031$), it is very difficult to disperse FG into the monomer. It is seen from the Figure 13 that using FG as filler, the degradation in the hardness of the PS/FG nanocomposite having maximum achievable value of ϕ is only 9%. At this value of ϕ, the composite possess the conductivity as high as 10^{-2} S/cm (Fig. 4). Probably the preparation technique i.e., *in situ* polymerization is responsible for comparatively lower decrease in the hardness as compared with other conventional composite fabricated via hot compression molding.[39]

CONCLUSIONS

The percolative nature of the insulator–conductor transition of PS/FG nanocomposite due to the addition of FG has been described by GEM equation. *In-situ* polymerization has resulted in the low value of volume fraction of FG for achieving percolation threshold. The electrical conductivity as high as 10^{-2} S/cm has been obtained without significantly affecting the hardness. High value of dielectric constant ($\sim 10^4$) has been obtained at low frequency for highly conducting PS/FG composite. The analysis of the current–voltage characteristics of PS/FG nanocomposite has revealed that the tunneling transport mechanism of charge carriers near the percolation threshold, transforms to ohmic conduction above percolation.

The authors are also grateful to Director, SSPL, Delhi for providing facilities for dielectric measurements.

References

1. Segal, E.; Tchoudakov, R.; Narkis, M.; Siegmann, A. J Mater Sci 2004, 39, 5673.
2. Hirano, S.; Kishimoto, A. Appl Phys Lett 1998, 73, 3742.
3. Ruschau, G. R.; Yoshikawa, S.; Newnham, R. E. J Appl Phys 1992, 72, 953.
4. Huang, J. C. Adv Polym Technol 2002, 21, 299.
5. Dong, Q.; Zheng, Q.; Zhang, M. J Mater Sci 2006, 41, 3175.
6. Celzard, A.; McRae, E.; Mareche, J. F.; Furdin, G.; Sundqvist, B. J Appl Phys 1998, 83, 1410.
7. Achour, M. E.; Malhi, M. E.; Miane, I. L.; Carmona, F.; Lahjomri F. J Appl Polym Sci 1999, 73, 969.
8. Yacubowicz, J.; Narkis, M. Polym Eng Sci 1990, 30, 459.
9. Chen, I. G.; Johnson, W. B. J Mater Sci 1991, 26, 1563.
10. Gokturk, H. S.; Fiske, T. J.; Kalyon, D. M. J Appl Polym Sci 1993, 50, 1891.
11. Chen, G. H.; Wu, D. J.; Weng, W. G.; He, B.; Yan, W. L. Polym Int 2001, 50, 980.
12. Chung, D. D. L. J Mater Sci 1987, 22, 4190.
13. Anderson, S. H.; Chung, D. D. L. Mater Res Soc Symp Proc 1983, 20, 271.
14. Foulger, S. H. J Appl Polym Sci 1999, 72, 1573.
15. Brandrup, J.; Immergut, E. H., Eds.; Polymer Handbook, 3rd ed.; Wiley: New York, 1989.
16. List of dielectric constant of materials on the website www.clippercontrols.com/info/dielectric_constants.html and www.timecal.com.
17. Wang, L.; Dang, Z. M. Appl Phys Lett 2005, 87, 042903.
18. Li, Y. J.; Xu, M.; Feng, J. Q. Appl Phys Lett 2006, 89, 072902.
19. Chen, G.; Weng, W.; Wu, D.; Wu, C.; Lu, J.; Wang, P.; Chen, X. Carbon 2004, 42, 753.
20. Sagalowicz, L.; Fox, G. R. J Mater Res 1999, 14, 1876.
21. Chen, G. M.; Liu, S. H.; Zhang, S. F.; Qi, Z. N. Macromol Rapid Commun 2000, 21, 746.
22. Kirkpatrik, S. Rev Mod Phys 1973, 45, 574.
23. Feng, J.; Chan, C. M. Polym Eng Sci 1998, 38, 1649.
24. Chen, X. B.; Devaux, J.; Issi, J. P.; Billaud, D. Polym Eng Sci 1995, 35, 637.
25. Rejon, L.; Zorala, A. R.; Calderon, J. P.; Castano, V. M. Polym Eng Sci 2000, 40, 2101.
26. Liu, Z.; Bai, G.; Huang, Y.; Feng, D.; Li, F.; Guo, T.; Chen, Y. Carbon 2007, 45, 821.
27. Wang, Y.; Rubner, M. F. Macromolecules 1992, 25, 3284.
28. Balberg, I.; Bozowski, S. Solid State Commun 1982, 44, 551.
29. McLachlan, D. S. J Phys C: Solid State Phys 1985, 18, 1891.
30. McLachlan, D. S. J Phys C: Solid State Phys 1987, 20, 865.
31. Straley, J. P. Phys Rev B 1977, 15, 5733.
32. Nakamura, S.; Saita, K.; Sawa, G.; Kitagawa, K. Jpn J Appl Phys 1997, 36, 5163.
33. Mamunya, Y. P.; Muzychenko, Y. V.; Pissis, P.; Lebedev, E. V.; Shut, M. I. Polym Eng Sci 2002, 42, 90.
34. Sichel, E. K.; Gittlemen, J. I.; Sheng, P. Phys Rev B 1978, 18, 5712.
35. Dang, Z. M.; Lin, Y. H.; Nan, C. W. Adv Mater 2003, 15, 1625.
36. Chiteme, C.; McLachlan, D. S. Phys Rev B 2003, 67, 024206.
37. Efros, A. L.; Shklovskli, B. I. Phys Stat Sol (b) 1976, 76, 475.
38. Dang, Z.; Shen, Y.; Fan, L.; Cai, N.; Nan, C. J Appl Phys 2003, 93, 5543.
39. Panwar, V.; Sachdev, V. K.; Mehra, R. M. Eur Polym J 2007, 43, 573.